Adv. Manuf. (2023) 11:56–74
https://doi.org/10.1007/s40436-022-00405-1

Exit morphology and mechanical property of FDM printed PLA: influence of hot melt extrusion process

Yan-Hua Bian[1,2,3] · Gang Yu[1,2,4] · Xin Zhao[3] · Shao-Xia Li[1,2] · Xiu-Li He[1,2] · Chong-Xin Tian[1,2] · Zhi-Yong Li[1,2]

Received: 26 June 2021 / Revised: 22 October 2021 / Accepted: 17 February 2022 / Published online: 10 August 2022

Abstract In order to study the hot melt extrusion process in fused deposition modeling (FDM), this study mainly explores the effects of printing temperature, heated block length, feeding speed on the exit morphology and mechanical properties of FDM printed Polylactic acid (PLA) samples. High-speed camera is used to capture the exit morphology of molten PLA just extruded to the nozzle. According to exit morphology, the outlet states of extruded molten material can be divided into four categories, namely, bubbled state, coherent state, expanding state, and unstable state. Tensile test results show that printing temperature, heated block length and printing speed have significant influence on tensile properties and fracture mode of FDM printed samples. When the heated block length is 15 mm and 30 mm, there is a ductile-brittle transition in fracture mode with the increase of printing speed. The printing process window under different heated block lengths and printing temperatures has been figured out and the distribution of printing process window under different printing speeds has been discussed. There is a maximum printing process window under the heated block length of 30 mm. This finding provides a frame work for performance prediction of FDM printed parts and theoretical guidance for expanding the scope of printing process window.

Keywords Fused deposition modeling (FDM) · Polylactic acid (PLA) · Exit morphology · Tensile property · Printing process window

1 Introduction

Fused deposition modeling (FDM), a fusion-extrusion based processing method, is one of the most widely used additive manufacturing (AM) technologies and can be used to manufacture complex components without other specialized tooling. FDM printed parts have been widely used in healthcare industry, food processing, aerospace, electronic production and so on [1–5]. In FDM process, thermoplastic polymers are delivered to the heated block through a feeding motor and selectively extruded on the platform according to planned path. Complex three-dimensional (3D) geometries, designed by a computer-aided design (CAD) program, can be modeled by the production mode of layer-by-layer accumulation. Through this process, several types of filament materials can be used to produce parts, such as polylactic acid (PLA), acrylonitrile butadiene styrene (ABS), polycarbonate (PC) and polyether ether ketone (PEEK). PLA with the advantage of biocompatibility, environmental degradability and low cost has become the most widely used material for FDM process. However, FDM-produced PLA parts also have the disadvantages of high brittleness, low deformation resistance temperature and poor consistency, which limits the possibility of FDM-produced PLA parts becoming the ultimate application products.

✉ Xiu-Li He
xlhe@imech.ac.cn

✉ Chong-Xin Tian
tianchongxin@imech.ac.cn

[1] Institute of Mechanics, Chinese Academy of Sciences, Beijing 100190, People's Republic of China

[2] School of Engineering Science, University of Chinese Academy of Sciences, Beijing 100049, People's Republic of China

[3] Research Institute of 3D Printing, Beijing City University, Beijing 100083, People's Republic of China

[4] Center of Materials Science and Optoelectronics Engineering, University of Chinese Academy of Sciences, Beijing 100049, People's Republic of China

Generally in FDM printing process, many parameters can affect the process of hot melt extrusion (HME) of material from heated block, crystallinity of extruded material and quality of layer-to-layer adhesion, and then affect the mechanical properties of FDM printed parts [6–8]. These parameters can be roughly divided into two categories: environmental parameters and structural parameters. Environmental parameters refer to the parameter set in printing process, including bed temperature, chamber temperature, printing temperature, cooling mode, printing speed, heated block length, nozzle diameter. Structural parameters are related to the structural strategy of printed parts, including extrusion multiplier, extrusion line width, build orientation, layer thickness, bottom solid layers, top solid layers, outline/perimeter, infill percentage, raster angle, air gap.

All these parameters can affect the mechanical properties of FDM printed parts in different ways. So far, the relationship between structural parameters, such as layer thickness [9–18], extrusion line width [11, 12, 18], build orientation [10, 13, 18–21], infill percentage [9, 16, 17, 21], raster angle [11, 13, 16], and the mechanical properties of molded parts have been extensively studied. Moreover, in order to improve mechanical properties, some researchers also optimize structural parameters in their studies [15, 22–24]. In Ref. [9], the experimental research showed that infill density had significant effect on modulus of elasticity, ultimate strength, and failure strain. Rahmati et al. [10] proposed a novel conservative failure model for FDM to provide underpredictions for the ultimate tensile strength and the correctness of the model was verified by PLA printed sample. Rajpurohit and Dave [13] studied the effects of raster angle, layer height, and raster width on the tensile properties of FDM printed PLA using an open-source 3D printer. They found that the sample built at 0° raster angle had higher ductility than that built at 45°and 90° raster angles. But there is no introduction of the parameters of the open-source 3D printer. It was seen in Ref. [15] that the PLA parts printed in x build orientation in a Cube 3D printer were stronger and more robust than the parts printed in y and 45° build orientations. They also found that the tensile strength of FDM printed sample was 60% higher than that of the raw filament material. Heidari-Rarani et al. [22] employed experiment method of Taguchi design to optimize FDM process parameters and predicted the mechanical properties of FDM printed samples. Liu et al. [18] applied the gray Taguchi method to optimize the mechanical properties of 3D-printed PLA part. They concluded that build orientation and layer height had significant effects on tensile strength, flexural strength and impact strength. Above research on structural parameters is mainly focused on the path planning in the printing process and its influence on mechanical property of the printed parts. However, during FDM process, property change of raw PLA on mechanical properties and exit morphology of molten PLA just extruded from the nozzle have not been fully investigated.

Among environmental parameters, printing temperature, printing speed, heated block length, and nozzle diameter are the main parameters affecting the HME process of material from heated block. Bed temperature, chamber temperature and cooling mode affect the thermal history of material in deposition process. In FDM printing process, the process of PLA filament heated into molten state in the heated block and extruded to the nozzle is the key to the whole printing process. The heating process of material in the heated block will greatly affect fluidity of the extruded material, continuity of extruded fibers, adhesion characteristics between layers, and then affect mechanical properties of the whole printed parts. The insufficient melting of PLA will make material block the nozzle, while the process of excessive melting will cause material carbonization. Efforts have been made to study the coalescence of filaments [7, 8, 25], the heat transfer [8, 26, 27] in attempt to enhance the understanding on the extrusion process in FDM printing process, but little attention has been paid to the flow state and rheological properties of material in the heated block. The development of new materials also needs a better understanding of the physics mechanism of material heating process in the heated block. Furthermore, according to the parameters provided by the material supplier, materials are allowed to be printed over a wide range of printing temperature, but the printability of material and the performance of molded parts vary greatly. The structure of heated block also affects the printability of the material and the mechanical properties of the printed parts. However, there were few researches on the effect of nozzle structure on hot melt process. Therefore, in order to meet the application requirements of final FDM products and promote the wider application of FDM technology, it is of great importance to investigate the influence mechanism of the HME process of PLA from the heated block on the mechanical properties thoroughly.

In this study, high-speed camera is used to capture the exit morphology of molten PLA just extruded from the nozzle. According to the exit morphology, the flow state of the molten PLA in the heated block is examined. Moreover, the influence mechanism of heated block length, printing temperature and printing speed on the mechanical property of FDM-produced PLA parts is investigated. This study aims to offer an insight into the relationship between the HME process of PLA being extruded from the heated block and the mechanical properties of the printed samples and provide a solution to expand the printing process window.

2 Experimental work

2.1 3D printer and material

As shown in Fig. 1, a self-developed 3D printer including mechanical structure, circuit control and thermal insulation shell was used in this study. The print head unit was mounted on two-axis CNC system in horizontal plane, so as to realize the two-dimensional movement. The printing platform with the size of 400 mm × 400 mm was mounted in z-direction and moved through a ball screw motor. The maximum printing height in z direction was 500 mm. The transmission accuracy of the machine in x–y direction was ±50 μm and ±10 μm in z direction. The material was supplied to the print head unit by a rolling wheel feeder via a long-range feeding pipe. The print head unit was mainly composed of a radiator, a heated block, a heated rod, a thermocouple sensor and a nozzle.

In the present research, PLA filaments (provided by Dongguan Making Top Electricity Technology Co., Limited, Guangdong, China) with a diameter of 2.85 mm, density of 1.24 g/cm^3, melting point of (210±8) °C and melt flow of 6 g/10 min was selected as the raw material.

2.2 Process for capturing exit morphology

The state of material in the heated block has an important effect on the mechanical properties of the printed parts, but it cannot be observed by direct methods. Therefore, in this paper, high-speed camera (i-speed210, iX Cameras, United Kingdom) was used for capturing exit morphology of the material just extruded to the nozzle and its installation was shown in Fig. 2. The high-speed camera was set with the frame rate of 500 per second and frame size of 1 488×1 054. Lighting equipment was used to provide strong light for the experimental process. Two computers were empolyed in the experiment, with one controlling high-speed camera and the other controlling printing temperature and feeding speed.

The parameter sets in the process to capture exit morphology are different from those in the printing process

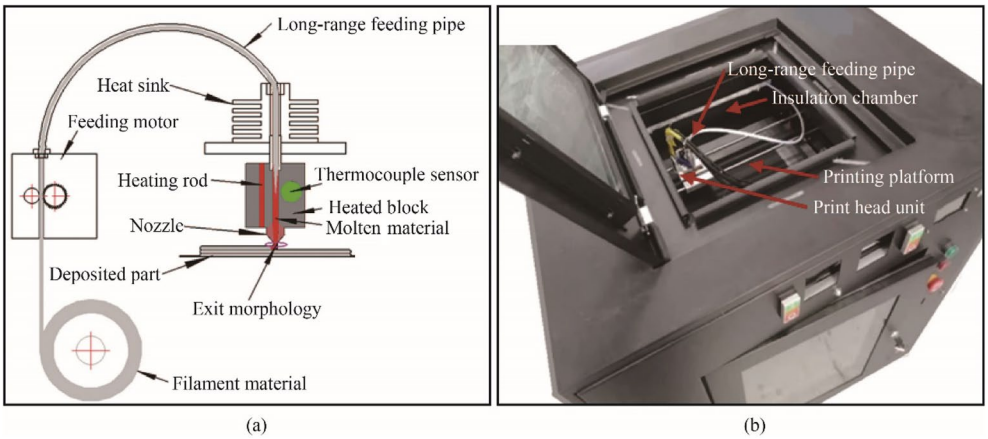

Fig. 1 **a** Schematic representation of 3D printer, **b** self-developed 3D printer

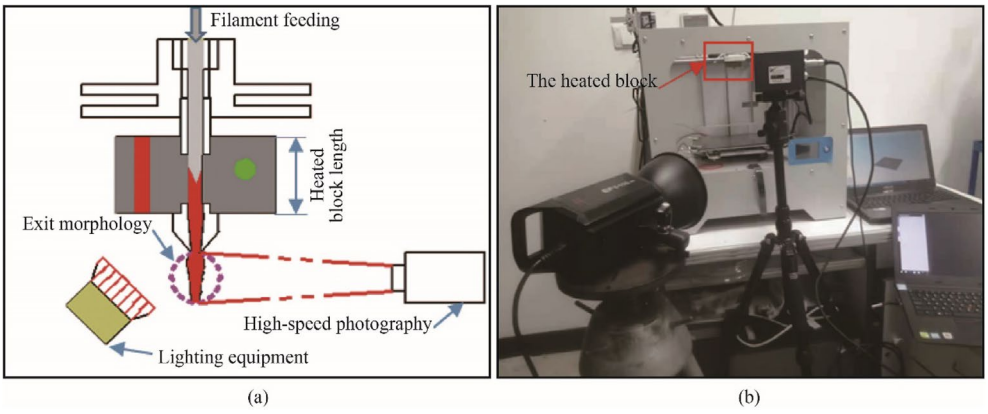

Fig. 2 **a** Schematic diagram, **b** experimental setup for capturing exit morphology

of FDM-produced samples. In the process to capture exit morphology, only the printing temperature and material feeding speed need to be set, and the feeding speed is determined by the rotational speed of the material feeding motor. In the printing process of FDM-produced samples, printing speed needs to be set. The printing speed is described by the movement speed of the two-axis CNC in horizontal plane, which is determined by many parameters such as extrusion multiplier, extrusion line width, feeding speed and filament diameter.

According to the law of mass conservation, the mass of the filament delivered to the heated block is equal to the deposition amount at the same time. As shown in Fig. 3, the relationship between material feeding speed and printing speed can be written as

$$Av_{xy}h_0l_w = \pi v_e\left(\frac{D}{2}\right)^2, \tag{1}$$

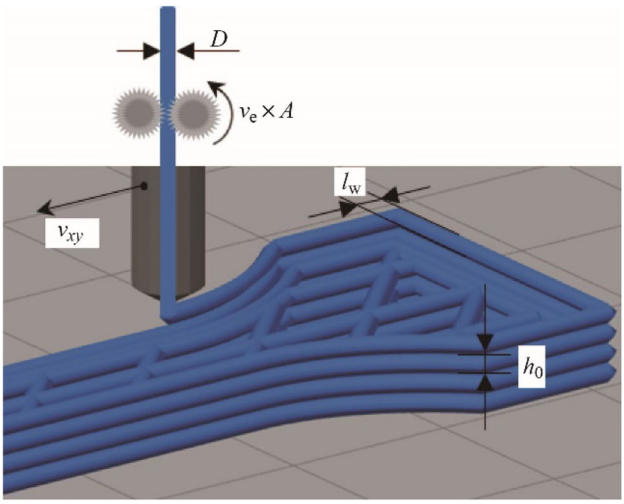

Fig. 3 Graphical representation of process parameters

$$v_e = \frac{4Av_{xy}h_0l_w}{\pi D^2}, \tag{2}$$

where v_e is the feeding speed of the material feeding motor, v_{xy} the printing speed of two-axis CNC in horizontal plane, h_0 the layer thickness, l_w the extrusion line width, D the filament diameter, A the extrusion multiplier. Here, A is used to compensate the error of feeding mass by proportional manner.

In this way, the filament feeding speed is characterized by printing speed.

2.3 Sample preparation

Tensile test specimens were designed according to the ISO 527-1:2012 standard [28]. Its two-dimensional diagram and tool path of FDM printing process were shown in Fig. 4. The directions of extruded fibers in the test sections were parallel to each other. The specimens were prepared with three printing temperature of 190, 210 and 230 °C and three different heated block length of 15, 30 and 60 mm. The printing speed was set from 10 mm/s to 90 mm/s with the increment of 10 mm/s. Under some combination of designed parameters, the maximum printing speed may not reach 90 mm/s. The fixed process parameters, such as interior fill percentage, layer thickness and substrate temperature, were shown in Table 1.

2.4 Tensile test machine and experimental set up

Tensile test was conducted using a universal testing machine (SANS, CMT5, MTS Industrial System, Shenzhen, China) with a load cell of 100 kN and an accuracy of ± 0.5%. The test was conducted at the temperature of 20 °C, relative humidity of 5%, and loading speed of 5 mm/min. Five specimens were tested for each printing parameter set. After the tensile test, the fractured surface was examined using the high-precision measuring microscope (Dino-Lite AM4115ZT), which has a magnification range from ×20 to ×220.

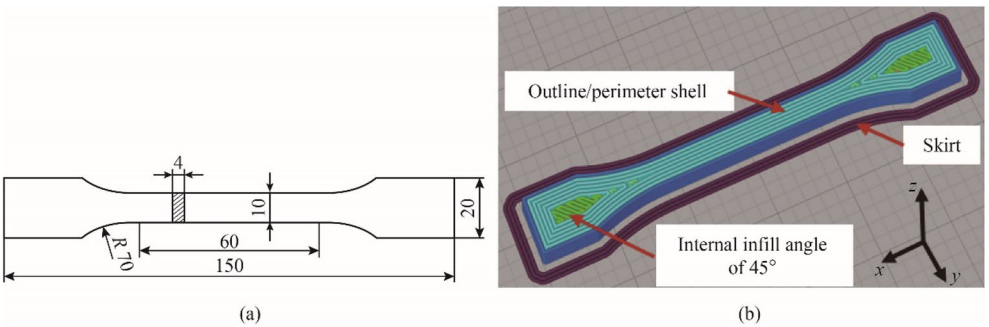

Fig. 4 Standard specimens for tensile test **a** two-dimensional diagram (all the dimension is in mm), **b** tool path of FDM printing process

Table 1 Fixed parameters and their values

Fixed parameters in printing process	Values
Nozzle diameter/mm	1
Extrusion multiplier	1.1
Extrusion line width/mm	1.2
Layer thickness/mm	0.5
Filament diameter/mm	2.85
Top solid layers	1
Bottom solid layers	5
Outline/perimeter shells	5
Skirt layers	1
Skirt offset from part/mm	2
Skirt outlines	3
Interior fill percentage/%	20
Outline overlap/%	20
Substrate temperature/°C	80

3 Results and discussions

3.1 Exit morphology of material extruded to the nozzle

The flow state of PLA material heated to molten state in the heated block would affect the exit morphology of molten material just extruded to the nozzle, and then affect the mechanical properties of the molded parts. Therefore, high-speed camera was used to capture the exit morphology, and the exit morphology was used to determine the state of molten PLA in the heated block. The heated block length, printing temperature and feeding speed are important physical parameters affecting the heat transfer process in the heated block and then affect the mechanical properties of FDM printed parts to a great extent. Figures 5–7 show the exit morphology under different heated block lengths, printing temperatures and feeding speeds. It is shown that the exit morphology can be divided into four categories: bubbled state, coherent state, expanding state and unstable state. For the bubbled state, there are many bubbles in the extruded molten material. For the coherent state, the diameter of extruded material is approximately coherent to nozzle diameter. For the expanding state, there is an inflation trend, which leads to larger diameter of molten material than nozzle diameter. For the unstable state, the diameter of extruded material is not uniform and the flow direction of the material is uncertain. The reason is that the shear force of molten materials is different in different positions inside the heated block, which causes the melt fracture or melt fracture tendency at the nozzle outlet.

Figure 5 shows the exit morphology under different feeding speeds at the heated block length of 15 mm under the printing temperature of 190, 210, 230 °C. In the experiments, the maximum feeding speed of filament material is 7 mm/s at the printing temperature of 210 °C and 230 °C, 6 mm/s at the printing temperature of 190 °C. When the maximum feeding speed is reached, the filament feeding device cannot work normally. The reason is that the force of filament acting as push rod is less than the reaction force of the molten material, resulting in the uneven restoring force of the melt PLA in all directions, and then the melt fracture tends to occur in the extruded material. When the printing temperature is 190 °C and the feeding speed is 1–2 mm/s, the width of the extruded material is stable and almost consistent with the nozzle diameter, namely the extruded molten material is in coherent state. When the feeding speed is 3–4 mm/s, the extruded material is much wider than the nozzle, namely the extruded molten material is in expanding state. When the feeding speed is 5–6 mm/s, the width of the extruded material fluctuates, indicating that the molten material inside the heated block is in an unstable flow state. This is due to the different shear forces in all directions when the molten material is extruded, and there is the melt fracture in the extruded material. When the printing temperature is 210 °C, the filament material has undergone the morphology evolution of bubbled state, coherent state, expanding state, unstable state, successively. The corresponding feeding speed is 1, 2–3, 4–5 and 6–7 mm/s. When the printing temperature is 230 °C, the feeding speed is 1 mm/s. There are a large number of bubbles in the extruded molten material, which will seriously affect the mechanical properties of FDM-produced parts.

Figure 6 shows the exit morphology under different feeding speeds at the heated block length of 30 mm. It can be seen from Fig. 6 that when the printing temperature is 190, 210, 230 °C, the maximum feeding speed is 6, 7 and 9 mm/s, respectively. At certain printing temperature, the filament material does not necessarily undergo all four morphology states. When the heated block length is 15 mm and 30 mm, and the printing temperature is 190 °C, there is no bubbled state. When the printing temperature is 230 °C and the feeding speed is 1 mm/s (as shown in Fig. 6c), there are a lot of bubbles in the extruded material and the extruded molten material fibers are discontinuous. The range of feeding speed corresponding to the coherent state is 3–5 mm/s and the range of feeding speed corresponding to the expanding state is 7–8 mm/s. When the feeding speed is 9 mm/s, there is obvious melt fracture phenomenon at the exit position of molten material.

Figure 7 shows the exit morphology under different printing speeds at the heated block length of 60 mm. It can be seen from Fig. 7 that under different printing temperatures, the maximum feeding speed is 9 mm/s. The relationship between feeding speed and printing speed is shown in Section 2.2. When the parameters used in the printing process are determined, there is a unique relationship between feeding speed and printing speed. It can be seen from Eqs.

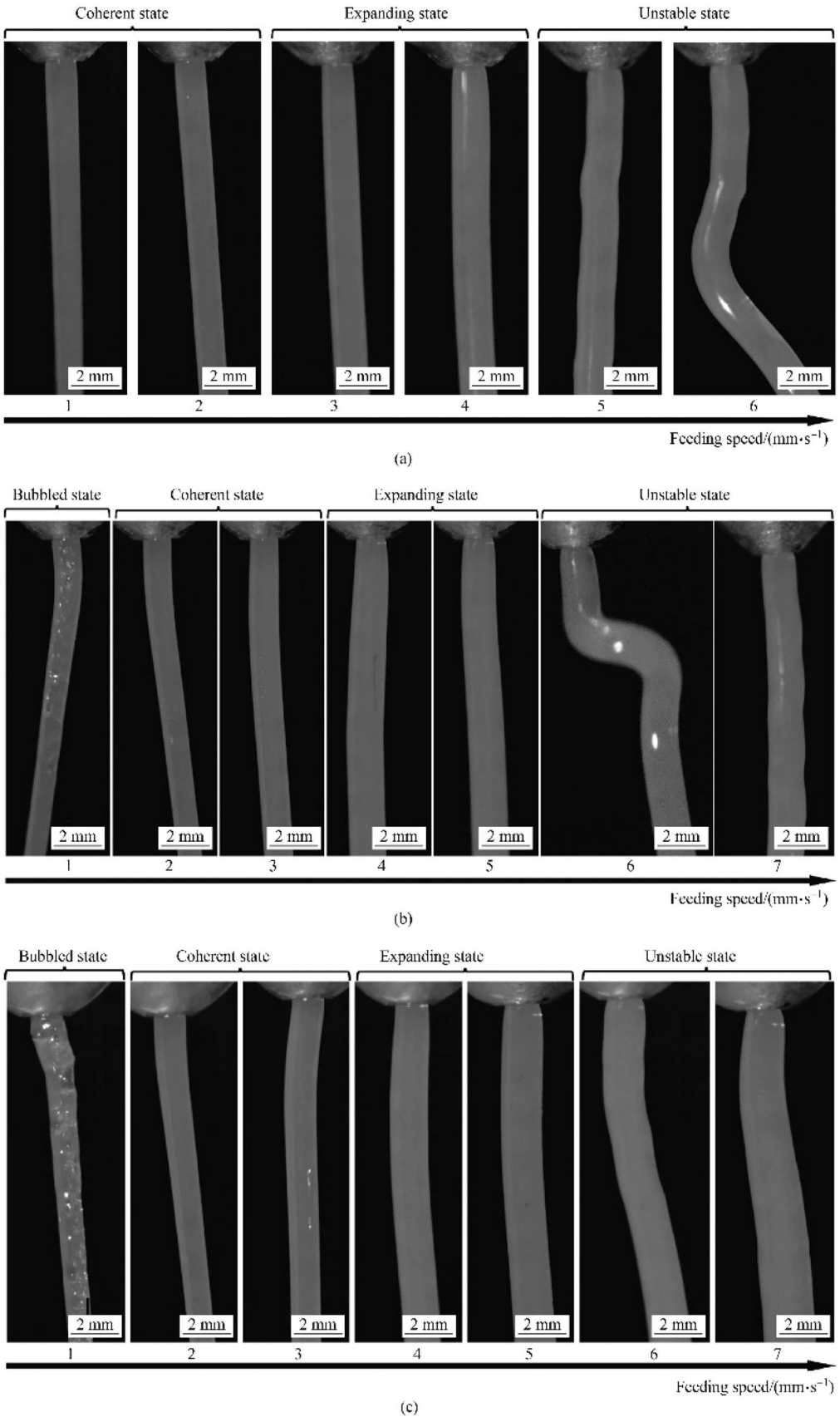

Fig. 5 Exit morphology under different feeding speeds at heated block length of 15 mm, printing temperatures of **a** 190 °C, **b** 210 °C, **c** 230 °C

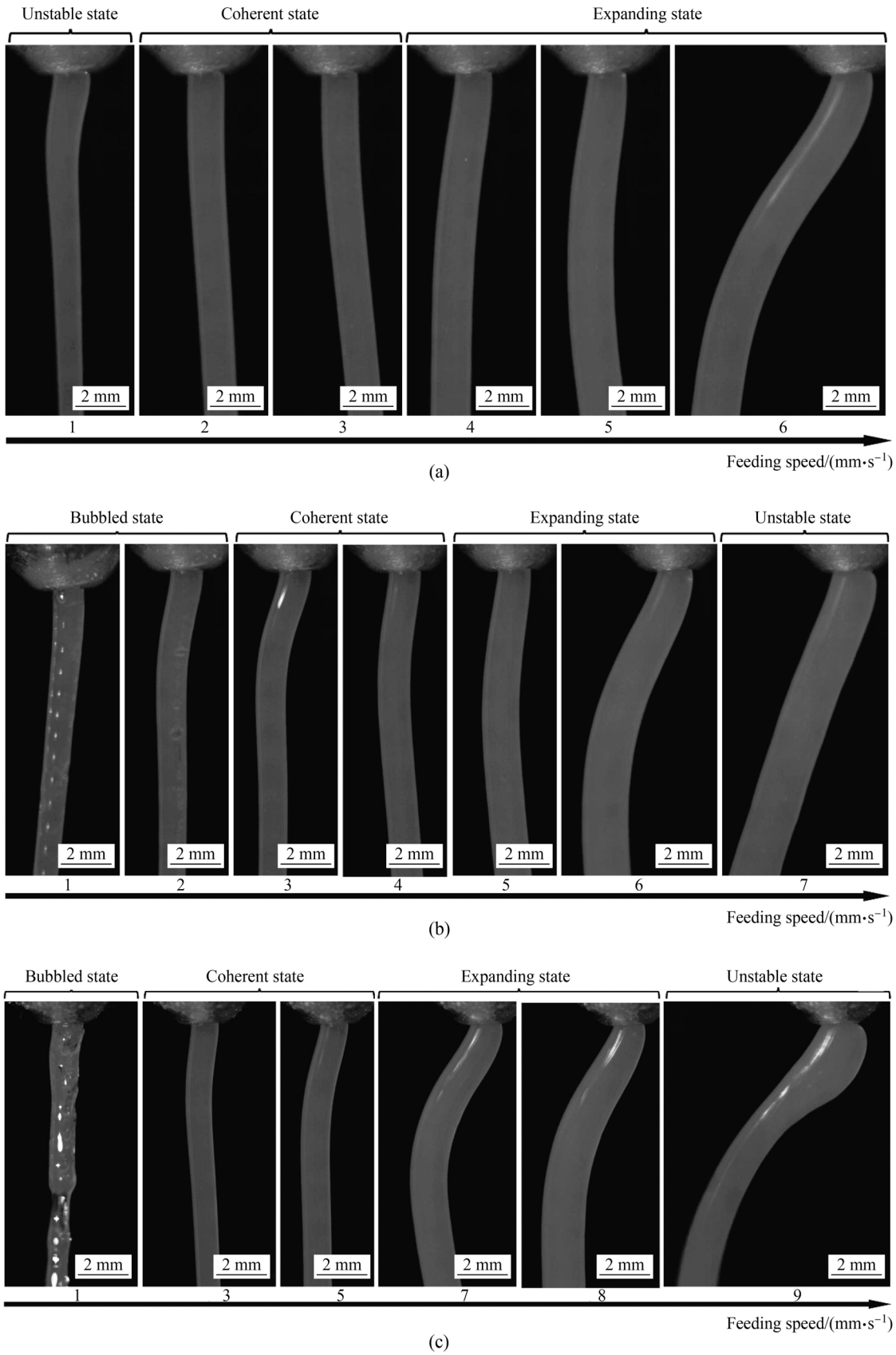

Fig. 6 Exit morphology under different feeding speeds at heated block length of 30 mm, printing temperatures of **a** 190 °C, **b** 210 °C, **c** 230 °C

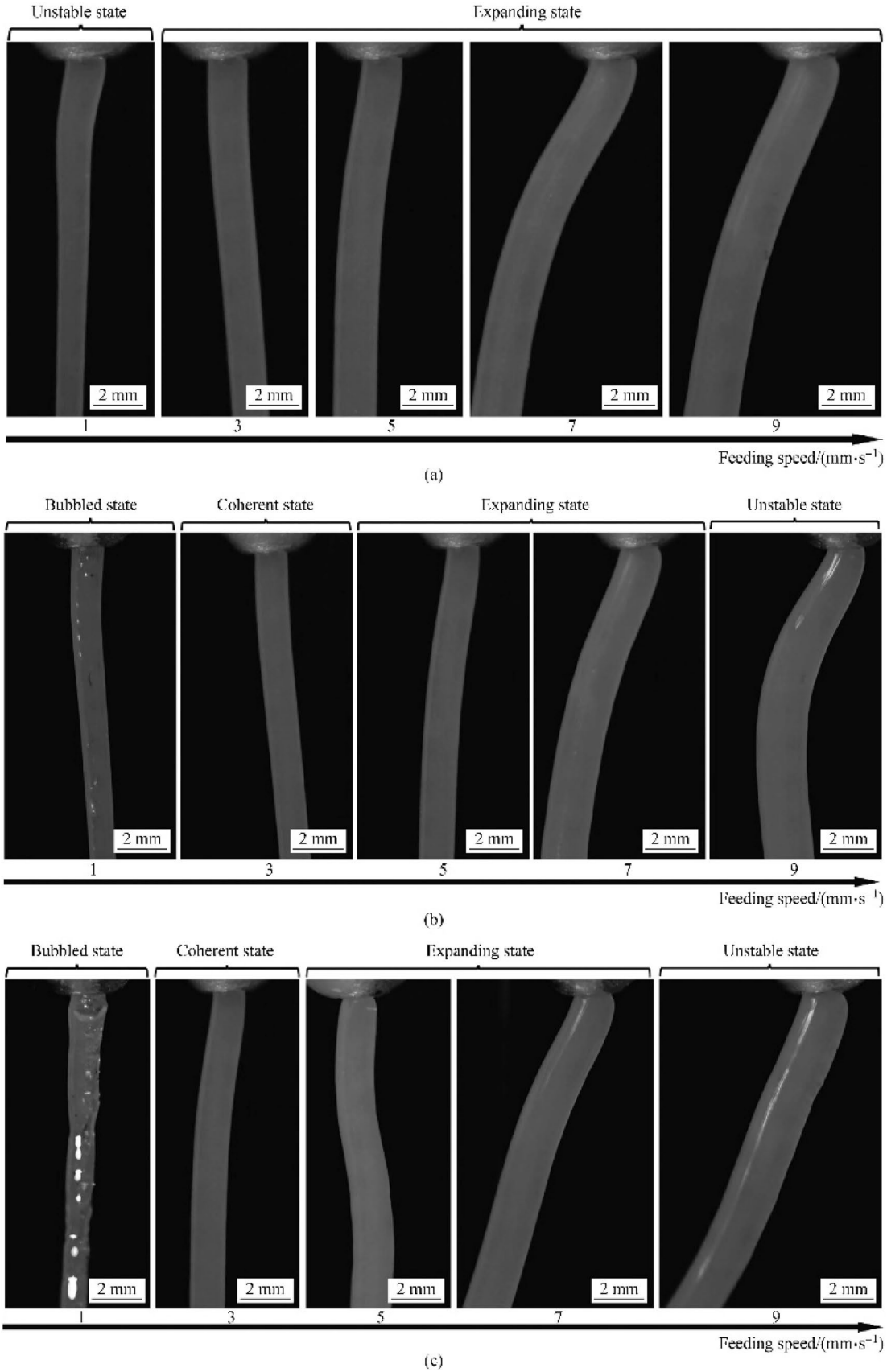

Fig. 7 Exit morphology under different feeding speeds at heated block length of 60 mm, printing temperatures of **a** 190 °C, **b** 210 °C, **c** 230 °C

(1) and (2) that there is a proportional linear relationship between feeding speed and printing speed. The maximum material feeding speed determines the maximum printing speed, and then determines the efficiency of printing process. Considering the maximum feeding speed, the printing efficiency is the highest under the heated block length of 60 mm. But the influence of the HME process of PLA from the heated block on the mechanical properties is still uncertain. When the printing temperature is 210 °C, the range of feeding speed corresponding to the state of exit morphology is similar with that under the printing temperature of 230 °C. The difference is that under the feeding speed of 1 mm/s and printing temperature of 230 °C, there are much more bubbles in the extruded material than those under the printing temperature of 210 °C.

As can be seen from Figs. 5–7, the influence of hot melt process of PLA in the heated block on the exit morphology is mainly represented in three aspects: the diameter of the extruded material, the extrusion direction and whether there are bubbles in the extruded material. When the printing temperature is 190 °C, there tends to be free of bubbles in the extruded PLA. During the extrusion process, uneven diameter of the extruded material easily results in defects such as holes inside the PLA parts. Furthermore, the use of extrusion parameters leading to outlet rupture should be avoided to prevent printing failure.

State diagram for exit morphology at heated block lengths of 15, 30 and 60 mm is shown in Fig. 8. The number in Fig. 8 is the maximum diameter of extruded PLA fiber in the expanding state. The flow pattern and stress of molten PLA in the heated block are shown in Fig. 9.

According to force analysis of melt in Fig. 9c, the forces acting on the molten PLA are in equilibrium

$$\sum F = F_1 + F_2 + F_3 = 0, \tag{3}$$

where F_1 is the resistance of the melt at the outlet, F_2 the resistance of surrounding melt, F_3 the thrust of the melt at the inlet.

$$F_3 = \dot{m} v_e, \tag{4}$$

where $\dot{m}$ is the feeding mass of filament PLA per unit time.

The shear stress τ_r acting on the melt is [29, 30]

$$\tau_r = \frac{r}{2R}\left(\frac{F_3 - F_1}{S}\right), \tag{5}$$

where r is the location radius of the melt, R the radius of the flow channel in the heated block, S the cross-sectional area of the melt element.

The velocity of melt flow v_r is [29, 30]

$$v_r = \left(\frac{n}{n+1}\right)\left(\frac{F_3 - F_1}{2\mu L S}\right)^{\frac{1}{n}}\left(R^{\frac{n+1}{n}} - r^{\frac{n+1}{n}}\right), \tag{6}$$

where L is the length of the flow channel, μ viscosity of the melt, n Non-Newtonian index.

When the molten PLA flows in the heated block, elastic energy will be stored, which is manifested as melt expansion at the outlet of the nozzle. With the increase of the heated block length, the feeding speed range for the exit morphology in expanding state is enlarged (as shown in Fig. 8).

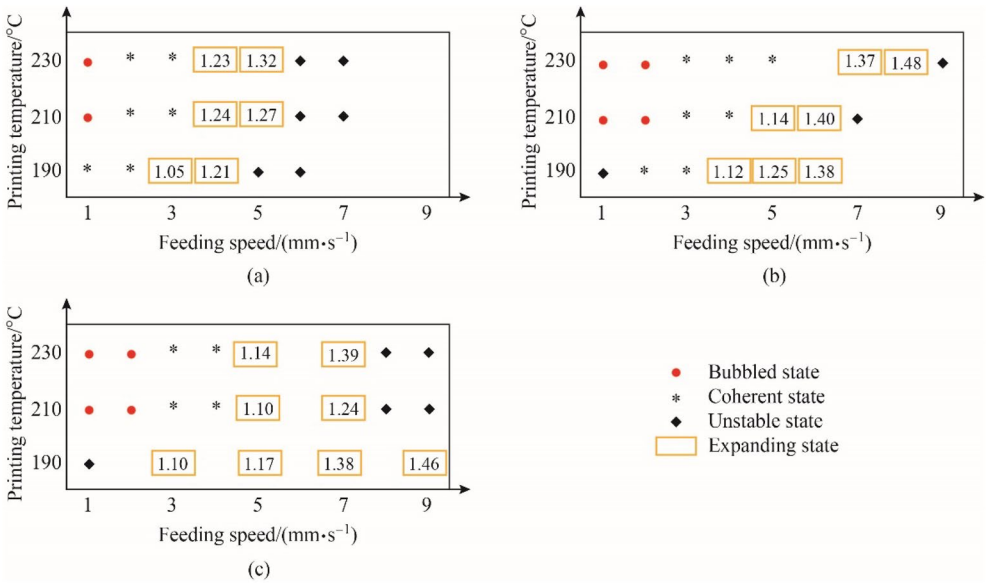

Fig. 8 State diagram for exit morphology at heated block lengths of **a** 15 mm, **b** 30 mm, **c** 60 mm

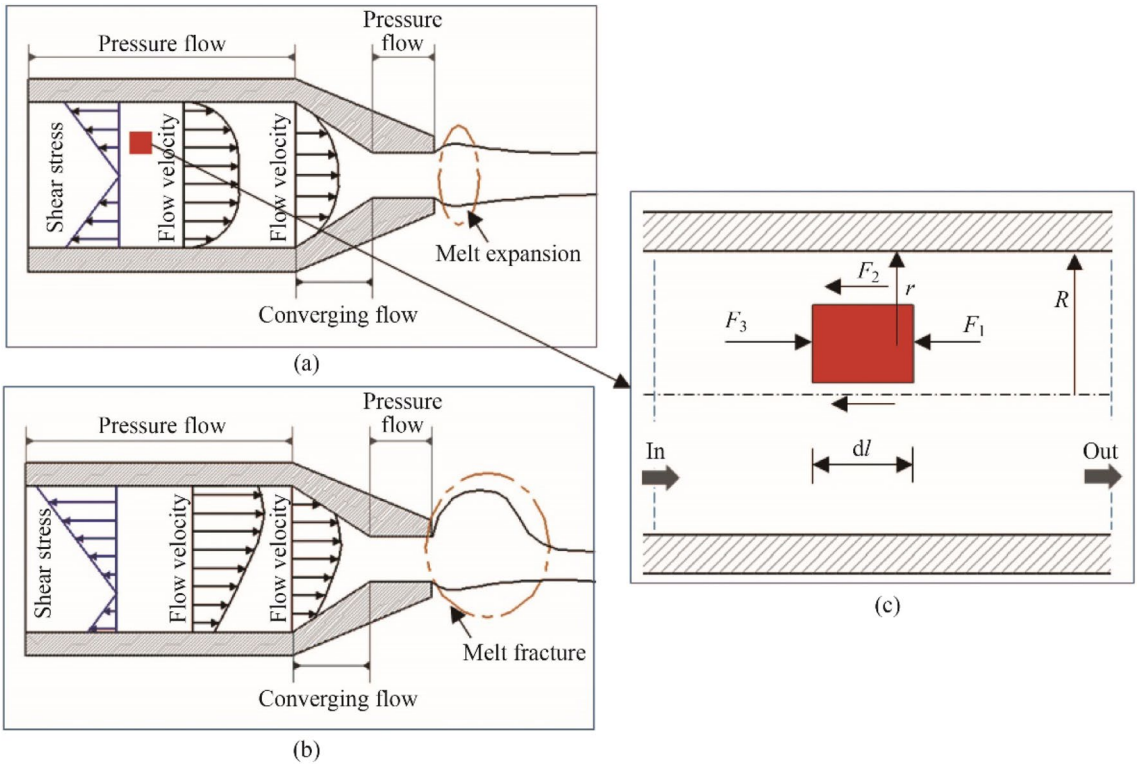

Fig. 9 Flow and force analysis of molten PLA in the heated block **a** steady flow, **b** unsteady flow, **c** force analysis of molten material

With the increase of feeding speed v_e, the thrust F_3 and the shear stress τ_r increase. There are more elastic deformation and elastic energy of molten PLA in the area with large shear stress. The uneven distribution of elastic energy in molten PLA leads to inconsistent elastic stress in the direction parallel to velocity of molten PLA. And the inconsistent elastic stress causes the disturbance in the molten PLA and then the flow in the heated block becomes unstable. When the melt flow in the heated block is unstable, the extruded PLA fiber is characterized by rough surface, uneven diameter, and wavy or periodic spiral in shape.

When the value of F_3 calculated from Eq. (4) is greater than the maximum force exerted by the filament feeding motor, the feeding motor cannot work normally and the feeding mass of filament cannot be guaranteed according to the printing parameters. At this time, the instability of melt flow in the heated block will increase. Therefore, the feeding speed is directly related to the maximum force exerted by the filament feeding motor when it is in unstable state according to exit morphology.

This study gives an insight into the application of high-speed camera for capturing the exit morphology of molten PLA extruded to the nozzle. The in-depth analysis of exit morphology may provide theoretical guidance for the selection of printing process parameters and the design of heated block.

3.2 Tensile property

In order to study the influence mechanism of the HME process of material extruded from the heated block on mechanical properties of FDM printed parts, the standard samples were printed at different heated block lengths, printing speeds and printing temperatures, and tensile tests were carried out. The mechanical properties such as ultimate tensile strength (UTS), elastic modulus and elongation at break can be obtained from the tensile stress-strain curve.

Generally, the tensile stress-strain process of polymer materials includes five stages: elastic deformation, yield strain softening, cold drawing, strain hardening and fracture (shown in Fig. 10 curve (b)), and not all polymer materials go through all of the five stages in tensile process. According to the stress-strain curve of tensile test, the fracture mode can be mainly divided into four modes [31, 32]. Figures 11–13 show the tensile stress-strain curves and typical fracture morphology of FDM printed samples in tensile test under the heated block length of 15, 30, and 60 mm, respectively. On the whole, the fracture modes of FDM produced samples include the malleability fracture, ductile fracture and brittle fracture.

When the heated block length is 15 mm (see Fig. 11), there is a transition from brittle fracture to ductile fracture

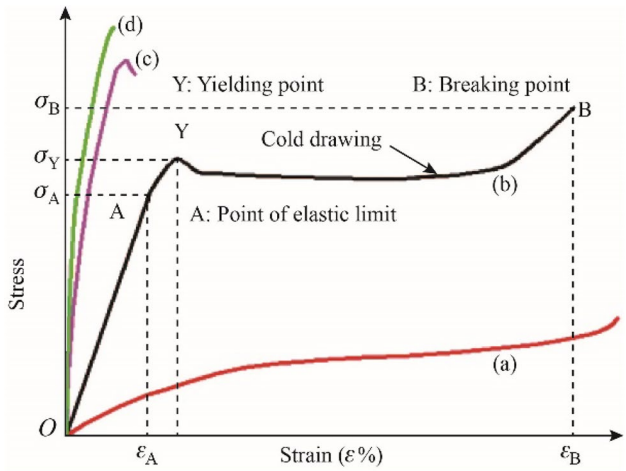

Fig. 10 Typical tensile stress-strain diagram of polymer

with the change of printing speed in the tensile test. Previous studies have shown that the heating process of PLA in the heated block has great influence on the crystallinity, and crystallinity of the material is the key factor to determine the mechanical properties of printed parts [33, 34]. When the printing speed and printing temperature is 50 mm/s and 190 °C, 10 mm/s and 210 °C, the fracture mode is brittle. Under the other condition, the fracture mode is malleable or ductile. It can be clearly seen from the tensile stress-strain curve shown in Fig. 11 that there is a cooling stage during the tensile test process under certain combinations of printing temperature and printing speed, such as the printing temperature of 190 °C and printing speed of 40 mm/s. When there is a cold drawing process, it indicates that the samples printed with parameter combination have the characteristic of toughness enhancement. Under different printing temperatures, the variation of the UTS with printing speed is not consistent. When the printing temperature is 190 °C, the UTS decreases with the increase of printing speed. When the printing speed increases, the hot melting time of raw filament in the heated block is reduced and there tends to be insufficient melt of raw filament in the heated block, resulting in high viscosity and poor fluidity of the extruded PLA fiber. As a result, the adhesion between layers of the printed part is reduced. On the other hand, under high speed printing, the extruded molten fiber is rapidly stretched, which may lead to insufficient time for the extruded molten fiber to bond with the cured fibers of upper layer. As a result, it can weaken the characteristics of interlayer bonding. At the same time, the cross section of the stretched molten PLA fiber becomes smaller, resulting in many holes in the fracture section of the tested sample.

When the printing temperature is 210 °C and 230 °C, the UTS increases first and then decreases. The maximum UTS is 63.5, 70.4 and 72.5 MPa and the corresponding printing temperatures and printing speeds are 190 °C and 10 mm/s, 210 °C and 40 mm/s, 230 °C and 10 mm/s, respectively. With the increase of printing temperature, the hot melting process of PLA material in the heated block becomes more sufficient, resulting in enhancement of melt fluidity of the extruded fiber, obvious overlap of adjacent fibers and reduction of the hole in cross section of the printed parts. However, when the printing temperature is too high, the molecular chain of PLA material can be degraded by effect of thermal oxidation, which can greatly decrease the mechanical properties of the printed parts.

When the heated block length is 30 mm, the fracture mode is mainly malleable or ductile. As can be seen from Figs. 12a–c, there are seven samples, whose elongations at break are greater than 5%, and there is an obvious cold drawing stage during tensile stress-strain process, the corresponding printing temperatures/printing speeds are: 190/20, 190/30, 210/40, 210/50, 210/60, 230/50, 230 °C/70 ($mm{\cdot}s^{-1}$). In those groups of process parameters, the material is heated uniformly in the heated block, and the flow is stable after extrusion. Under the printing temperature of 190 °C, the maximum elongation at break is 6.45%. At this time, the printing speed is 30 mm/s. When increasing the printing temperature to 210 °C and 230 °C, the elongation at break is 4.12% and 4.35%, respectively. The brittleness of printed parts can be enhanced by increasing printing temperature. When the printing temperature is 210 °C and 230 °C, the maximum elongation at break is 6.05% and 6.44%, and the corresponding printing speed is 40 mm/s and 70 mm/s, respectively. Increasing the printing speed can reduce the heating time of raw filament in the heated block, which can reduce the effect of high printing temperature on the brittleness of the printed part.

When the heated block is 30 mm, the variation of the UTS shows the similar rule with that for the heated block length of 15 mm under the same printing temperature. That is to say, when the printing temperature is 190 °C, the UTS decreases with the increase of printing speed. When the printing temperature is 210 °C and 230 °C, the UTS increases first and then decreases. The maximum UTS is different under different printing temperatures. When the printing temperatures are 190, 210, 230 °C, the maximum UTSs are 71.0, 75.8 and 74.5 MPa, respectively, and the corresponding printing speeds are 10, 40 and 50 mm/s, respectively. As can been seen from Fig. 12a, the elastic modulus decreases with the increase of printing speed under the printing temperature of 190 °C. However, the variation trend of elastic modulus with the printing speed is not obvious under other printing temperatures. This is due to the coupling effect of printing speed and printing temperature on the mechanical properties of the printed parts. Therefore, only under a reasonable combination

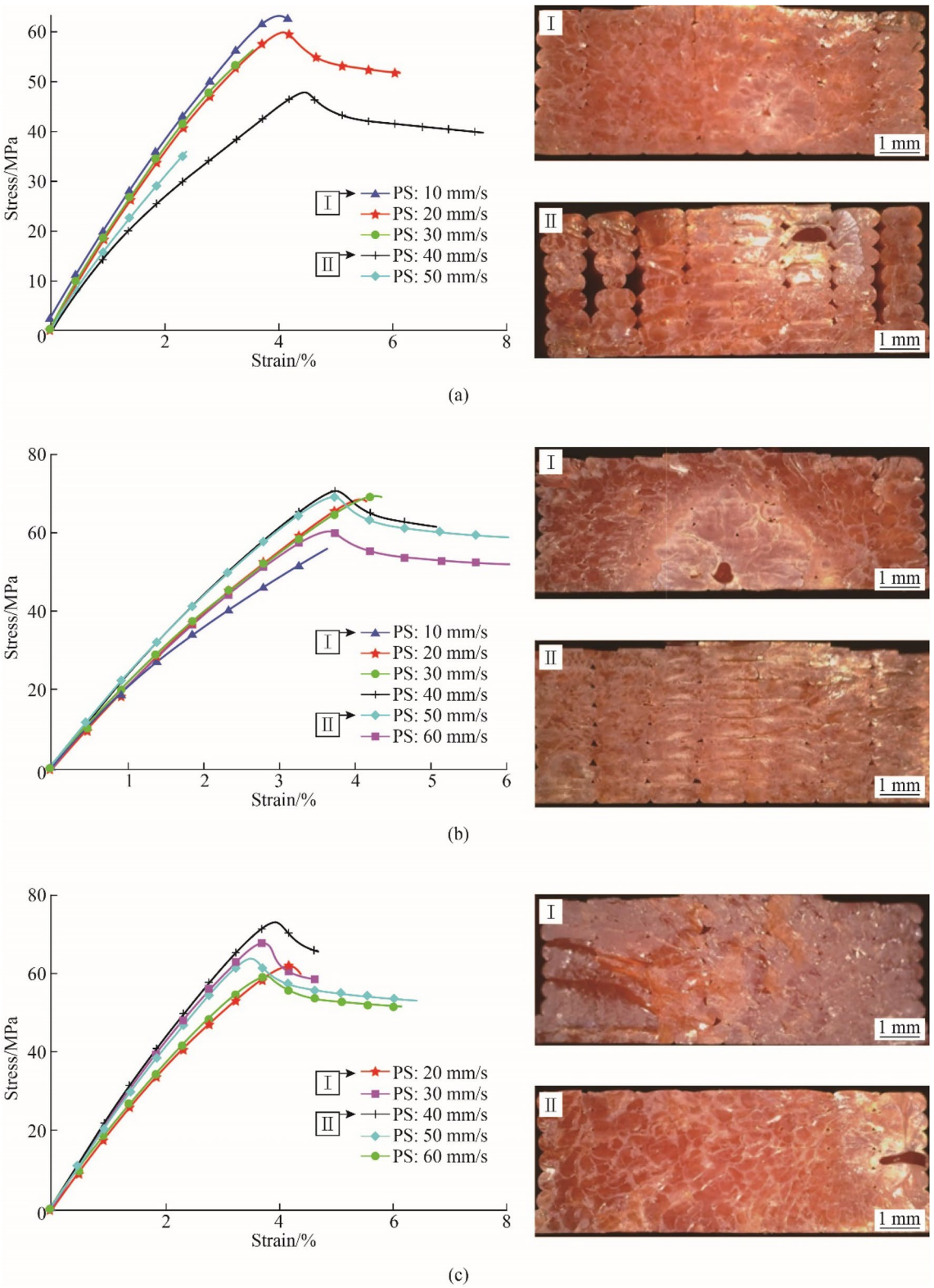

Fig. 11 Tensile stress-strain curve and fracture morphology at heated block length of 15 mm, printing temperatures of **a** 190 °C, **b** 210 °C, **c** 230 °C (PS: printing speed)

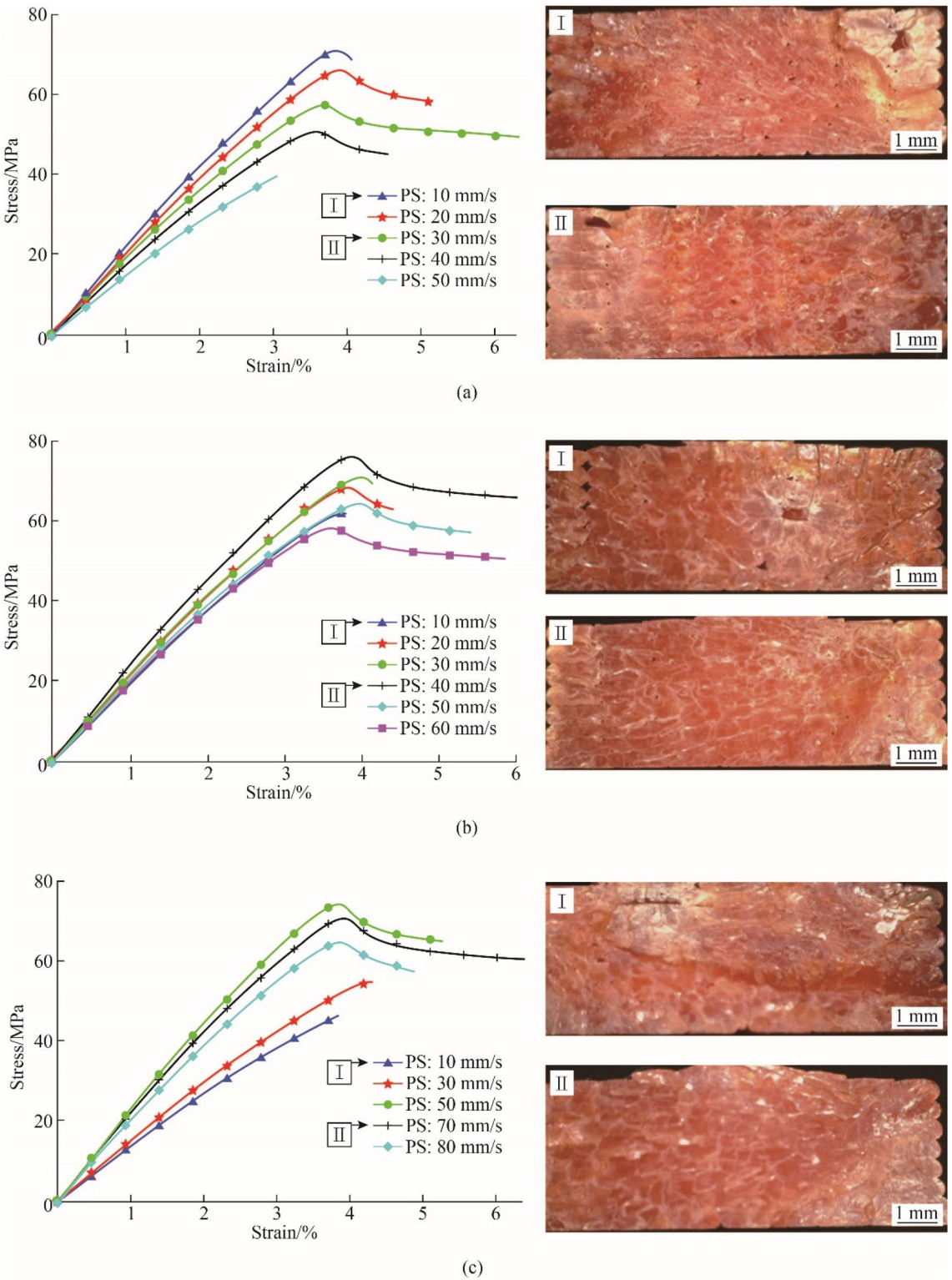

Fig. 12 Tensile stress-strain curve and fracture morphology at heated block length of 30 mm, printing temperatures of **a** 190 °C, **b** 210 °C, **c** 230 °C

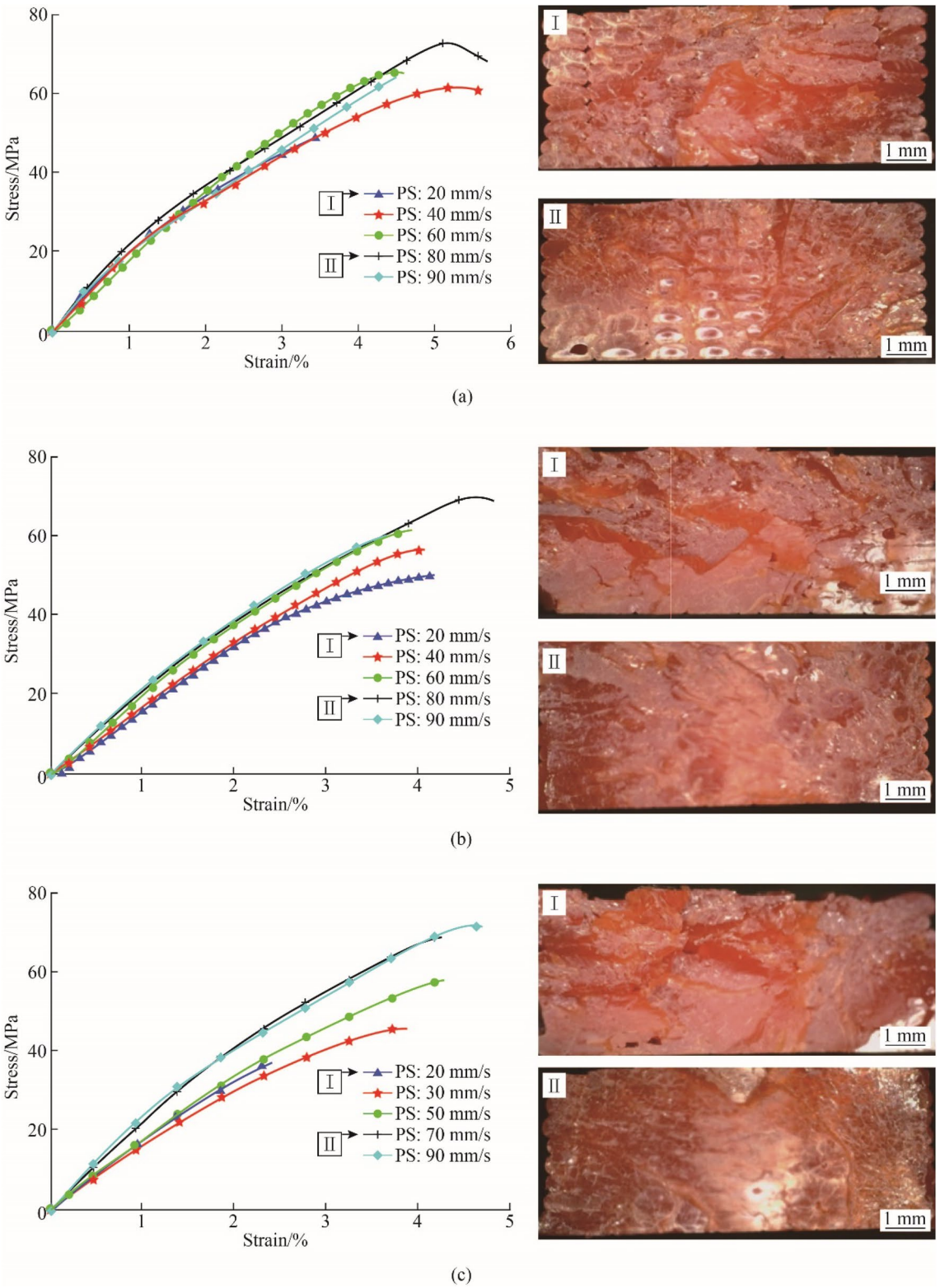

Fig. 13 Tensile stress-strain curve and fracture morphology at heated block length of 60 mm, printing temperatures of **a** 190 °C, **b** 210 °C, **c** 230 °C

of printing parameters, the mechanical properties such as UTS, elongation at break and elastic modulus of the printed parts can be optimized, and the combination of the optimized parameters is closely related to the structure of the heated block.

When the heated block length is 60 mm, almost all the samples show brittle fracture and FDM printed samples show the characteristic of softness and brittleness (see Fig. 13). The reason may be that with the increase of heated block length, the hot melt process for raw PLA filament is more complex with higher heating temperature and longer residence time, leading to the increase of brittleness after extrusion. When the printing temperature is 190 °C and 230 °C, the elongation at break is less than 5%. In all tensile tests, the minimum elongation at break is 2.4%, which occurs in two combination groups of 60 mm, 20 mm/s, 230 °C and 15 mm, 50 mm/s, 190 °C, but the reasons for these two parameter sets are different. The former is caused by the excessive melting of material, while the latter is due to the poor fusion of extruded materials, which induces poor bonding of molten PLA fibers. The maximum UTS is different under different printing temperatures. When the printing temperatures are 190, 210, 230 °C, the maximum UTSs are 72.7, 69.5, 71.5 MPa, respectively, and the corresponding printing speeds are 70, 70 and 90 mm/s, respectively.

Figures 11–13 also show the fracture morphology of typical tensile process. On the whole, the typical fracture morphology can be divided into three types.

(i) Dense surface with a few small voids and distinct extruded fiber shapes, such as I and II in Figs. 11b, I and II in Figs. 12a, and I in Fig. 13a.
(ii) Surface with many large voids, such as II in Fig. 11a.
(iii) Dense surface without extruded fiber shapes, such as II in Figs. 11c, I and II in Figs. 12c, and I and II in Fig. 13c.

When printing temperature is relatively low, the heated block length is relatively small, and the printing speed is relatively high, there are many large voids as shown in Figs. 11a II. Under this condition, the raw PLA filament is under-melting in the heated block, which will inevitably lead to weak adhesion of extruded fibers. The UTS of the corresponding samples, shown as II in Fig. 11a, is only 44.8MPa.

When printing temperature is relatively high and heated block length is relatively large, the fracture surface tends to be compact, which is accompanied by the disappearance of the extruded fibers boundary and the fusion between adjacent fibers. In this condition, the material in the heated block is over melted; the fracture mode tends to be brittle fracture; and the elongation at break is small. The elongation at break of the corresponding sample, shown as I in Fig. 13c, is only 2.4%.

3.3 Printing process window

The UTS is the maximum stress that material can withstand while being stretched or pulled. The UTS is calculated by dividing the cross-section area of the material tested by the stress placed on the material, generally expressed as pounds or tons per square inch. The UTS is an important standard to measure the application ability of materials under tensile load. As known from www.matweb.com/, the Ingeo™ 2002D Extrusion Grade PLA which is developed by NatureWorks® is widely used in many areas, with the UTS of 60.0 MPa, the tensile strength at break of 53.0 MPa. In this study, when the UTS is greater than 60 MPa, the combination of printing process parameters is regarded as the printing process window. As shown in Figs. 14a and 16a, the UTS is plotted as a function of printing temperature and printing speed under the heated block length of 15, 30 and 60 mm, respectively (see Fig. 15). The combination of process parameters with the UTS greater than 60 MPa is marked in Figs. 14a and 16b, and the shaded area represents the range of the printing process window. When the heated block length is 15 mm, the printing process window is the smallest. Under the heated block length of 60 mm, the UTS under low printing speed does not reach 60 MPa. The reason is that when the printing speed is low, the material in the heated block is over-melted, and there are many bubbles inside the molten material (as shown in Section 3.1). The heated block with the length of 60 mm is more suitable for high speed printing. Under the heated block length of 30 mm, the range of printing process window is the largest. Moreover, both high-speed and low-speed printing can be realized successfully by selecting appropriate printing temperature. As a result, the heated block length of 30 mm is more suitable for the printing process requirements of different 3D models.

The heated block length, printing temperature and printing speed will affect the HME process of PLA from the heated block. Experimental results show that the HME process of PLA from the heated block has a great influence on the mechanical properties of FDM printed samples. In this study, the printing process window under different heated block lengths and printing temperatures is obtained. On the premise of ensuring the mechanical properties of FDM printed parts, high-speed printing process is achieved, which is helpful to improve the efficiency of printing process. This study provides a solution for expanding the application field of FDM technology and making FDM printed parts meet the application requirements of final products.

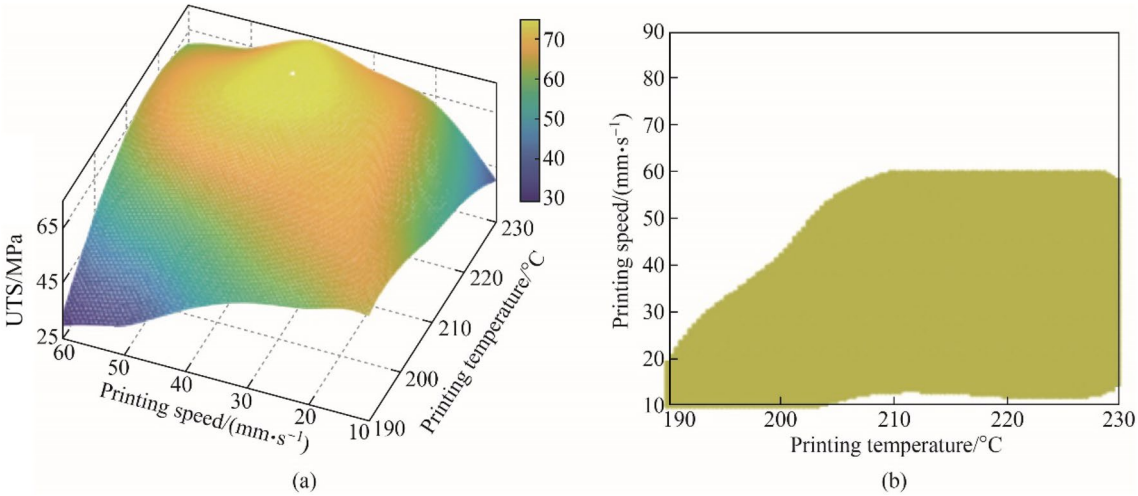

Fig. 14 UTS and printing process window under heated block length of 15 mm **a** UTS as a function of printing temperature and printing speed **b** printing process window

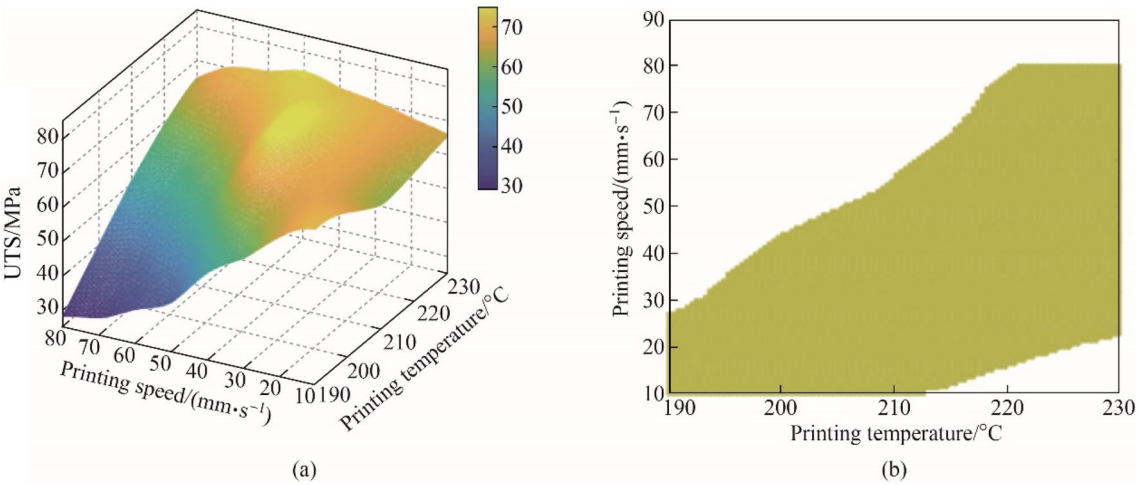

Fig. 15 UTS and printing process window under heated block length of 30 mm **a** UTS as a function of printing temperature and printing speed **b** printing process window

4 Conclusions

In this work, the exit morphology of molten PLA material has been obtained using high-speed camera. The effect of heated block length, feeding speed and printing temperature on the exit morphology of molten PLA material has been studied. The exit morphology is divided into four states: bubbled state, coherent state, expanding state, and unstable state. Different flow states affect the mechanical properties, fracture modes and printing process window of FDM produced parts to a certain extent.

The effects of different heated block lengths, printing speeds and printing temperatures on tensile properties of FDM produced parts have been studied. When the heated block lengths are 15, 30 and 60 mm, respectively, the maximum UTSs are 72.5, 75.8 and 72.7 MPa, under the printing temperatures and printing speeds of 230 °C and 10 mm/s, 210 °C and 40 mm/s, 190 °C and 70 mm/s. Both over-melting and under-melting of PLA in the heated block will lead to lower elongation at break.

According to the tensile stress-strain curves of FDM produced specimens, there are three types of fracture mode, namely, malleability fracture, ductile fracture and brittle fracture. When the heated block length is 60 mm, almost all samples exhibit brittle fracture. When the heated block lengths are 15 mm and 30 mm, there is ductile-brittle transition in fracture mode with the increase of printing speed. Longer heated block length, higher printing temperature,

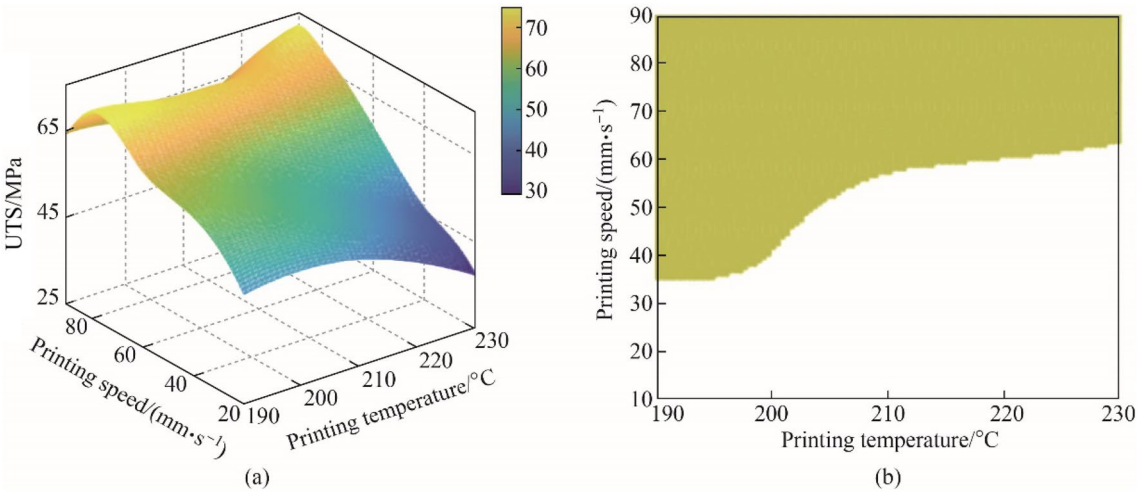

Fig. 16 UTS and printing process window under heated block length of 60 mm **a** UTS as a function of printing temperature and printing speed **b** printing process window

and lower printing speed lead to complex HME process with higher heating temperature and longer residence time of the raw PLA filaments in the heated block and cause the increase of brittleness of the extruded PLA. The fracture morphology is also affected by the HME process of PLA from the heated block.

The UTS greater than 60 MPa is considered as the standard to determine the printing process window. The heated block length affects the size and distribution of printing process window greatly. When the heated block length is 30 mm, the range of printing process window is larger than that for other heated blocks, which is more suitable for the requirements of printing different types of 3D models. It is conducive to the improvement of printing efficiency with the heated block length of 60 mm.

Acknowledgements This work was supported by the National Natural Science Foundation of China (Grant Nos. 11502269 and 11672304), and plan of Beijing Municipal Commission of Science and Technology (Grant No. Z181100003818015).

References

1. Feng X, Ma L, Liang H et al (2020) Osteointegration of 3D-printed fully porous polyetheretherketone scaffolds with different pore sizes. ACS Omega 5(41):26655–26666
2. Rodríguez-Parada L, Mayuet PF, Gámez AJ (2019) Evaluation of reliefs' properties on design of thermoformed packaging using fused deposition modelling moulds. Materials 12(3):478. https://doi.org/10.3390/ma12030478
3. Galatas A, Hassanin H, Zweiri Y et al (2018) Additive manufactured sandwich composite/ABS parts for unmanned aerial vehicle applications. Polymers 10(11):1262. https://doi.org/10.3390/polym10111262
4. Daneshmand S, Aghanajafi C (2012) Description and modeling of the additive manufacturing technology for aerodynamic coefficients measurement. Stroj Vestn J Mech E 58(2):125–133
5. Espalin D, Muse DW, Macdonald E et al (2014) 3D printing multifunctionality: structures with electronics. Int J Adv Manuf Tech 72(5/8):963–978
6. Yang C, Tian X, Li D et al (2017) Influence of thermal processing conditions in 3D printing on the crystallinity and mechanical properties of peek material. J Mater Process Tech 248:1–7
7. Sun Q, Rizvi GM, Bellehumeur CT et al (2008) Effect of processing conditions on the bonding quality of FDM polymer filaments. Rapid Prototyp J 14(2):72–80
8. Shelton TE, Willburn ZA, Hartsfield CR et al (2019) Effects of thermal process parameters on mechanical interlayer strength for additively manufactured Ultem 9085. Polym Test 81:106255. https://doi.org/10.1016/j.polymertesting.2019.106255
9. Heidari-Rarani M, Parisa S, Niloofar E (2020) Effect of processing parameters on tensile properties of FDM 3D printed of PLA specimens. J Sci Technol Compos 2(7):855–862
10. Rahmati A, Heidari-Rarani M, Lessard L (2021) A novel conservative failure model for the fused deposition modeling of polylactic acid specimens. Addit Manuf 48:102460. https://doi.org/10.1016/j.addma.2021.102460
11. Letcher T, Waytashek M (2014) Material property testing of 3D-printed specimen in PLA on an entry-level 3D printer. In: proceedings of the ASME 2014 international mechanical engineering congress and exposition. Volume 2A: Advanced Manufacturing. Montreal, Quebec, Canada. November 14–20, 2014. https://doi.org/10.1115/imece2014-39379
12. Peng A, Xiao X, Yue R (2014) Process parameter optimization for fused deposition modeling using response surface methodology combined with fuzzy inference system. Int J Adv Manuf Tech 73(1/4):87–100
13. Rajpurohit SR, Dave HK (2018) Analysis of tensile strength of a fused filament fabricated PLA part using an open-source 3D printer. Int J Adv Manuf Tech 101:1525–1536
14. Wang P, Zou B, Xiao H et al (2019) Effects of printing parameters of fused deposition modeling on mechanical properties, surface quality, and microstructure of peek. J Mater Process Tech 271:62–74

15. Chacón JM, Caminero MA, García PE et al (2017) Additive manufacturing of PLA structures using fused deposition modelling: effect of process parameters on mechanical properties and their optimal selection. Mater Des 124:143–157
16. Samykano M, Selvamani SK, Kadirgama K et al (2019) Mechanical property of FDM printed ABS: influence of printing parameters. Int J Adv Manuf Tech 102:2779–2796
17. Camargo JC, Machado LR, Almeida EC et al (2019) Mechanical properties of PLA-graphene filament for FDM 3D printing. Int J Adv Manuf Tech 103(5):2423–2443
18. Liu X, Zhang M, Li S et al (2017) Mechanical property parametric appraisal of fused deposition modeling parts based on the gray Taguchi method. Int J Adv Manuf Tech 89(5/8):2387–2397
19. Mst FA, Masood SH, Iovenitti P et al (2016) Effects of part build orientations on fatigue behaviour of FDM-processed PLA material. Prog Addit Manuf 1:21–28
20. Afrose MF, Masood SH, Nikzad M et al (2014) Effects of build orientations on tensile properties of PLA material processed by FDM. Adv Mat Res 1044/1045:31–34
21. Gonabadi H, Yadav A, Bull SJ (2020) The effect of processing parameters on the mechanical characteristics of PLA produced by a 3D FFF printer. Int J Adv Manuf Tech 111(3/4):695–709
22. Heidari-Rarani M, Ezati N, Parisa S et al (2020) Optimization of FDM process parameters for tensile properties of polylactic acid specimens using Taguchi design of experiment method. J Thermoplast Compos Mater 3:1–18
23. Zhou X, Hsieh SJ, Wang JC (2019) Accelerating extrusion-based additive manufacturing optimization processes with surrogate-based multi-fidelity models. Int J Adv Manuf Tech 103(1):4071–4083
24. Panda SK, Padhee S, Sood AK et al (2009) Optimization of fused deposition modelling (FDM) process parameters using bacterial foraging technique. Intell Inf Manag 1(2):89–97
25. Gurrala PK, Regalla SP (2014) Part strength evolution with bonding between filaments in fused deposition modelling. Virtual Phys Prototyp 9:141–149
26. Costa SF, Duarte FM, Covas JA (2015) Thermal conditions affecting heat transfer in FDM/FFE: a contribution towards the numerical modelling of the process. Virtual Phys Prototyp 10:35–46
27. Heidari-Rarani M, Rafiee-Afarani M, Zahedi AM (2019) Mechanical characterization of FDM 3D printing of continuous carbon fiber reinforced PLA composites. Compos B Eng 175:107147. https://doi.org/10.1016/j.compositesb.2019.107147
28. Standards B (2012) Plastics-determination of tensile properties-Part 1: general principles (ISO 527-1:2012). CEN/TC 249-Plastics
29. Roger TF (1979) Principles of polymer processing. The Macmician Press Ltd., London. https://doi.org/10.1007/978-1-349-16234-5
30. Zehev T, Costas GG (1979) Principles of polymer processing. Wiley, New York. https://doi.org/10.1002/aic.690260135
31. Bower DI (1981) An Introduction to polymer physics. Cambridge University Press, Cambridge
32. Ward IM, Sweeney J (2013) Mechanical properties of solid polymers, 3rd edn. Wiley, New York
33. Shibata M, Inoue Y, Miyoshi M (2006) Mechanical properties, morphology, and crystallization behavior of blends of poly(l-lactide) with poly(butylene succinate-co-l-lactate) and poly(butylene succinate). Polymer 47(10):3557–3564
34. Pillin I, Montrelay N, Grohens Y (2006) Thermo-mechanical characterization of plasticized PLA: is the miscibility the only significant factor? Polymer 47(13):4676–4682

Yan-Hua Bian is a Ph.D. candidate at the Institute of Mechanics, Chinese Academy of Sciences, China. Her research interests include additive manufacturing, fused deposition modelling and selective laser melting.

Gang Yu is a professor at the Institute of Mechanics, Chinese Academy of Sciences, China. He received his Ph.D. from Heriot-Watt University, the United Kingdom. His research focuses on laser advanced manufacturing and additive manufacturing technology.

Xin Zhao is an associate professor at Research Institute of 3D printing, Beijing City University, China. His research interests include additive manufacturing, fused deposition modelling and inkjet 3D printing technology.

Shao-Xia Li is an associate professor at the Institute of Mechanics, Chinese Academy of Sciences, China. She holds a Ph.D. from the Institute of Mechanics, Chinese Academy of Sciences, China. Her research interests include additive manufacturing and laser surface modification.

Chong-Xin Tian is an assistant professor at the Institute of Mechanics, Chinese Academy of Sciences, China. His research interests include additive manufacturing and surface nanocrystallization of materials.

Xiu-Li He is an associate professor at the Institute of Mechanics, Chinese Academy of Sciences, China. She received her Ph.D. from the Pennsylvania State University, the United States. She is engaged in the research of additive manufacturing, welding and joining, and computational materials processing.

Zhi-Yong Li is an assistant professor at the Institute of Mechanics, Chinese Academy of Sciences, China. His research interests include additive manufacturing, welding and joining.